Acuity-independent effects of visual deprivation on human visual cortex

Chuan Hou[a,b,1], Mark W. Pettet[c], and Anthony M. Norcia[d]

[a]Department of Ophthalmology and Ophthalmic Laboratory of Vision Research, State Key Laboratory of Biotherapy, West China Hospital, Sichuan University, Chengdu 610041, China; [b]The Smith-Kettlewell Eye Research Institute, San Francisco, CA 94115; [c]Department of Psychology, University of Washington, Seattle, WA 98195; and [d]Department of Psychology, Stanford University, Stanford, CA 94305

Edited by J. Anthony Movshon, New York University, New York, NY, and approved June 23, 2014 (received for review March 7, 2014)

Visual development depends on sensory input during an early developmental critical period. Deviation of the pointing direction of the two eyes (strabismus) or chronic optical blur (anisometropia) separately and together can disrupt the formation of normal binocular interactions and the development of spatial processing, leading to a loss of stereopsis and visual acuity known as amblyopia. To shed new light on how these two different forms of visual deprivation affect the development of visual cortex, we used event-related potentials (ERPs) to study the temporal evolution of visual responses in patients who had experienced either strabismus or anisometropia early in life. To make a specific statement about the locus of deprivation effects, we took advantage of a stimulation paradigm in which we could measure deprivation effects that arise either before or after a configuration-specific response to illusory contours (ICs). Extraction of ICs is known to first occur in extrastriate visual areas. Our ERP measurements indicate that deprivation via strabismus affects both the early part of the evoked response that occurs before ICs are formed as well as the later IC-selective response. Importantly, these effects are found in the normal-acuity nonamblyopic eyes of strabismic amblyopes and in both eyes of strabismic patients without amblyopia. The nonamblyopic eyes of anisometropic amblyopes, by contrast, are normal. Our results indicate that beyond the well-known effects of strabismus on the development of normal binocularity, it also affects the early stages of monocular feature processing in an acuity-independent fashion.

visual deficits | V1 | extrastriate cortex | visual processing | human electrophysiology

Over 50 y of research on experimental animal models has indicated that deprivation of normal visual experience during a developmental critical period perturbs both the structure and function of primary visual cortex (1–4). The animal models were developed to understand the underlying neural mechanisms of amblyopia, a common human developmental disorder of spatial vision associated with the presence of strabismus, anisometropia, or form deprivation during early life (5). Amblyopia is classically defined on the basis of poor visual acuity, but many other visual functions are known to be affected (6–8).

The earliest experimental studies of visual deprivation focused on the effects of monocular lid suture, and these studies showed devastating effects on the ability of the deprived eye to drive neural responses, retain synaptic connections, and guide visual behavior (9–11). Later work studied less extreme forms of deprivation that are common in humans, such as the effects of strabismus (deviation of the pointing direction of the two eyes) (12, 13) or anisometropia (chronic optical blur) (14, 15). More recent studies (16, 17) have found that losses in cell responses in primary visual cortex appear to be insufficient to explain the magnitude of behaviorally measured deficits. Based on these results, a hypothesis has been put forward that these forms of deprivation have their primary effects in extrastriate cortex (16).

Motivated by this idea, psychophysicists have sought evidence that extrastriate cortex is particularly impaired in human amblyopia. This work has used tasks whose execution is fundamentally limited by processing resources that single-cell physiology suggests are located in extrastriate cortex. As a second step, these studies have scaled stimuli based on visual acuity and compensated for contrast sensitivity losses to equate the output of early visual cortex from the amblyopic eye to that of normal-vision participants. Despite a nominal match at the level of early visual cortex outputs, patients with amblyopia still show deficits on illusory tilt perception (18), contour integration (19–23), global motion sensitivity (8, 24–28), object enumeration (29), and object tracking (7, 30). The impairments listed above have been interpreted to indicate that amblyopia may involve abnormalities in "higher-level" (e.g., extrastriate) neural processing that occur independent of any deficits in early processing stages (e.g., in striate cortex). A limitation of the existing psychophysical approaches has been the need to make an assumption that the stimulus scaling used to equate stimuli for visibility fully equilibrates the activity of early visual cortex. It would be preferable to take an approach that allows one to measure neural responses directly from both early and later stages of visual processing. Here we use event-related potentials (ERPs) and a stimulation paradigm that allow us to record responses from both early visual cortex and higher-level, extrastriate areas.

Our approach is similar in spirit to existing psychophysical approaches: We use a stimulus configuration—illusory contours (ICs)—that previous single-unit studies have shown to be first extracted in extrastriate cortex (31–34). ICs, also referred to as subjective contours, render object borders that are perceptually vivid but that are created in the absence of luminance contrast or chrominance gradients (35). ICs have been widely used to study

Significance

Deviation of the direction of two eyes (strabismus) or chronic optical blur (anisometropia) separately and together can disrupt the development of visual cortex. To shed new light on how these two forms of visual deprivation affect cortical development, we used event-related potentials coupled with a stimulation paradigm to study the temporal evolution of visual responses in patients who had experienced either strabismus or anisometropia early in life. Our results indicate that strabismus generates significant abnormalities at both early and later stages of cortical processing and, importantly, that these abnormalities are independent of visual-acuity deficits. The nonamblyopic eyes of anisometropic amblyopes, by contrast, are normal, suggesting that these two forms of visual deprivation are differentiated very early in visual cortex.

Author contributions: C.H. and A.M.N. designed research; C.H. performed research; M.W.P. contributed new reagents/analytic tools; C.H. analyzed data; and C.H. and A.M.N. wrote the paper.

The authors declare no conflict of interest.

This article is a PNAS Direct Submission.

[1]To whom correspondence should be addressed. Email: chuanhou@ski.org.

This article contains supporting information online at www.pnas.org/lookup/suppl/doi:10.1073/pnas.1404361111/-/DCSupplemental.

mechanisms of scene segmentation and grouping operations that are among the most fundamental tasks the visual system has to perform (36). ICs have garnered considerable interest because of their "inferential" nature—despite the lack of luminance edges, the visual system uses implicit configural cues to infer the presence of a contour. Finally, behavioral investigations in macaque suggest that IC perception is strongly dependent on higher visual areas, including V4 (37, 38) and inferotemporal (IT) cortex (39, 40).

Instead of attempting to equate the visibility of stimuli in the amblyopic eye to that of normal control eyes, as has been typical practice in the study of amblyopia, we make a close analysis of the effects of deprivation that is based on ERP responses from the nonamblyopic eyes of patients with anisometropic or strabismic amblyopia. These eyes have normal visual acuity and normal or even supernormal contrast sensitivity (41), making the stimuli nominally equivisible without the need for scaling. We then measure evoked responses at early latencies before the time that IC selectivity arises to assess the integrity of early visual cortex, and compare these responses to those measured at longer latencies after robust IC selectivity has been established. Previous single-unit studies that have used ICs of the type used in the present study indicate that they are first extracted no later than V2 (31, 42, 43) or V4 (34). Given the difference in species and stimuli, we will refer in the following to evoked responses that lack IC sensitivity as having arisen in "early" visual cortex, rather than in specific visual areas. To further specify the site of deprivation effects, we also study a group of stereo-blind patients with strabismus who do not have amblyopia (normal visual acuity in each eye).

A second goal of our study is to compare the effects of deprivation from unilateral blur (anisometropia) to that caused by strabismus. The human psychophysical literature has made a distinction in the pattern of visual loss associated with strabismus versus that associated with anisometropia (44). At least some of the differences in performance between these two types of deprivation can be explained on the level of residual stereopsis, which typically differs between these two populations (41). Whenever these two types of deprivation have been compared in terms of their effects on the monocular cell properties of V1, there has been little to differentiate the effects of the two types of deprivation (16, 45, 46). Unfortunately, there are relatively few studies of the effects of critical period deprivation on the cell-tuning properties in extrastriate cortex of any species (15, 17, 47), and there has been no comparison of the effects of strabismus vs. anisometropia in extrastriate cortex. The implication of the existing animal literature is that strabismus and anisometropia have comparable effects on early visual cortex and thus the divergence in their behavioral phenotype, as well as the major effects of deprivation, will lie in extrastriate cortex. Here we show that these two types of deprivation have differential effects very early in visual cortex, possibly as early as the transfer of information from V1 to V2.

Results

Specific ERP Responses to Illusory Contours. A large-field, repetitive IC display was used to enhance response amplitudes and to reduce the requirements on strict fixation of a small region (see Fig. 1*A* for an illustration of the full display in the IC-present state). Each inducer comprised a notched circle. When the inducers align with the rectangular lattice underlying the pattern, a percept of multiple illusory rectangular figures is present. This image was alternated with a second image, in which each of the inducers was misaligned by a 50° rotation about the center so as to disrupt the percept of the illusory figures. These two image states were presented for 500 ms in alternation (1 Hz; Fig. 1*B*, *Upper*, test condition). As a control for the contribution of local contrast and motion cues to the ERP, responses were measured to a display that had the same number of inducers undergoing an equivalent amount of angular rotation (e.g., 50° of rotation between offsets of 20° and 70° vs. 50° of rotation between offsets of 0° and 50° as in the test condition; Fig. 1*B*). To minimize the effects of reduced acuity in the amblyopic eyes of the patients, we used low-spatial frequency, high-contrast inducers (see details in *Materials and Methods*).

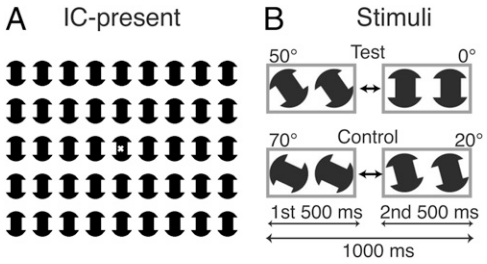

Fig. 1. Schematic illustrations of the stimuli used in the experiments. (*A*) The display comprised 45 notched-circle inducers. In the IC-present state, the inducers were aligned (0°), creating the percept of a set of illusory rectangles. The x in the center of the display indicates the fixation point. (*B*) ERP responses were measured under two conditions: a test condition in which the inducers alternated between a misaligned state (50°, IC-absent, the first 500 ms) and an aligned state (0°, IC-present, the second 500 ms), and a control condition in which the alternation was between two IC-absent misaligned states (70°, the first 500 ms and 20°, the second 500 ms). The motion cue due to rotation was the same (50°) in both test and control conditions.

The alternation between the aligned and misaligned inducer states created a robust percept of the appearance and disappearance of rectangular illusory figures, whereas the alternation between the two misaligned inducer states did not. For simplicity, we only plot the ERP responses after the second transition for both test and control conditions (Fig. 2), as this transition had the most comparable orientation of the inducers (0° vs. 20°) and because it highlights responses to perceptually different states (IC-present vs. IC-absent). In each case, there had been a preceding 50° rotation of the inducers, and thus the local transients and rotational motion cues were equated.

Both test and control conditions evoked an initial positive response between ∼70 and 115 ms with a peak around 100 ms (marked "P1"), followed by a negative response (between ∼120 and 220 ms) with a peak around 170 ms (marked "N1") and a late response (∼230–400 ms; marked "L") in all three groups: normals (normal observers), anisometropic amblyopia (aniso-amblyopia), and strabismic amblyopia (strab-amblyopia). IC-selective responses were defined as a differential response to test vs. control conditions. In Fig. 2, the black dots (bolded sections) on the waveforms indicate the time points that were significantly different between the test and the control condition on permutation testing with a run-corrected P value of less than 0.05 (48). The N1 and L components were significantly larger in the IC-present condition than in the IC-absent condition in the dominant eye of each group and were also significantly different on the trailing edge of the P1 component, starting at ∼110 ms in the normal group. We consider these larger P1, N1, and L components to be "IC-selective responses" because they occur after the onset of the configuration that supports IC perception but not after an equivalent local change in the inducers. The IC effect was significant at all active electrode derivations. The data in Fig. 2 are from the O_2 electrode (right hemisphere), where the responses to the IC stimulus were largest among five active electrode derivations (PO_7, O_1, O_Z, O_2, and PO_8). Larger, right-hemisphere IC-selective responses with similar timing have been reported previously in normal-vision participants (49, 50).

Response Abnormalities in Both Amblyopic and Dominant Eyes of Patients. In contrast to normal-acuity eyes, IC-selective responses were not measurable in the amblyopic eyes of both aniso- and

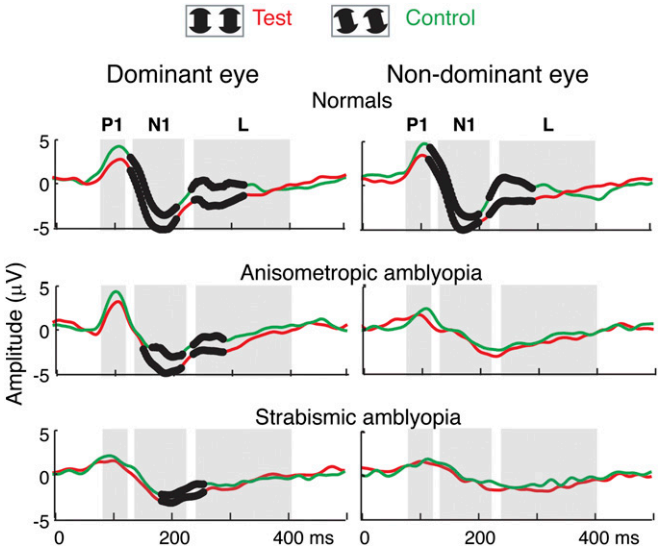

Fig. 2. Comparison of evoked responses between test (IC-present; red curves) and control (IC-absent; green curves) conditions in the same eye. The responses were averaged from each group (n = 10) at the O_2 derivation. Black dots (bolded sections) on the waveforms indicate the time points that were significantly different between the test and the control conditions on permutation testing ($P < 0.05$). IC-selective responses are defined here as a differential response to test vs. control conditions. In the normal-vision participants, IC selectivity is first seen around 110 ms on the downward slope of the P1 response peak and continues through the N1 and L time periods (gray bands) in both eyes. In the patients with anisometropic amblyopia, IC selectivity is present with a slight delay in the dominant eye but is not measurable in the nondominant, amblyopic eye. An IC-selective response is present with a delay in the dominant eye of the patients with strabismic amblyopia but not in their nondominant, amblyopic eye.

strab-amblyopes (Fig. 2, *Right*). Instead, amblyopic eyes showed reduced and delayed responses to both test and control conditions relative to their dominant eyes and both eyes of normals. It is also apparent from inspection of Fig. 2 that the dominant-eye response of the participants with strabismic amblyopia differs from those of both normal and aniso-amblyopic participants, despite the fact that all these eyes have equivalent visual acuity. To show this more clearly, we replot the data from Fig. 2, comparing the waveforms across participant groups (Fig. 3*A*). The response from the dominant eyes of the anisometropic participants is very similar to that of the normal controls, but the response from the dominant eyes of strabismic patients is depressed—despite their normal visual acuity. One can also see that the magnitude of the differences between eyes and conditions is reduced in the participants with strabismus.

To capture the full multivariate structure across the two stimulus conditions, two tested eyes, and three participant groups, we used partial least squares (PLS) regression to reduce the dimensionality of the data (51). PLS generates spatiotemporal response components that reflect the combination of factors in the experimental design, independent of any prior identification of specific components, such as at P1 or N1 (see details in *Materials and Methods*). This analysis allowed us to quantify multivariate differences between groups, eyes, and stimuli at all time points while controlling for multiple comparisons. PLS yielded two significant latent variables (LVs) ($P < 0.0001$). The time courses for each LV are shown in Fig. 3*B* (*Left*), with time points of significant multivariate difference highlighted by black dots. The LV "design" weights associated with each condition are shown (Fig. 3*B*, *Right*). The pattern of the first LV weights indicates that both eyes of the normals and the dominant eye of anisometropic amblyopes performed similarly in both test and control conditions—the weights for each of these eyes are all strongly positive, and more so in the test than in the control condition (Fig. 3*B*, *Upper*). By contrast, the weight of the dominant eye of the participants with strabismic amblyopia is negative, as is the weight for amblyopic eyes in the test and control conditions. Thus, the response pattern in the dominant eye of the patients with strabismic amblyopia more closely resembles that of amblyopic eyes than of the dominant eyes of normals or participants with anisometropic amblyopia. This pattern of difference was associated with significant differences during the time of the P1 and N1 peaks and during the time of the L peak. The multivariate difference, which presents as early as ~100 ms, is maximal between ~150 and 200 ms. This result is surprising, because the dominant eyes of the patients with strabismic amblyopia have normal levels

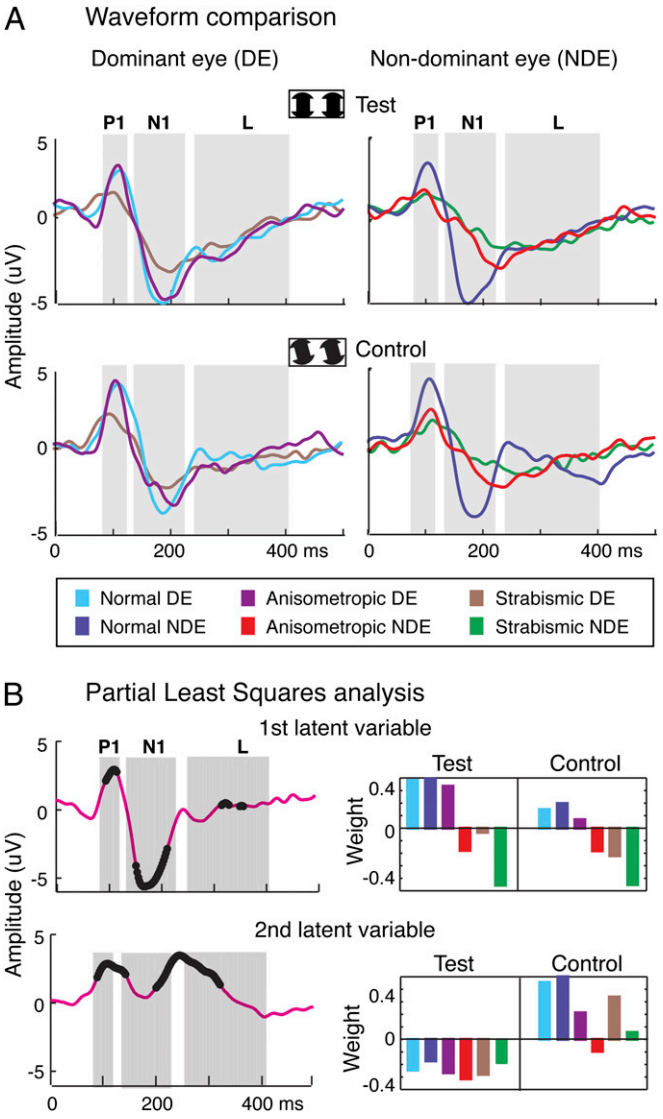

Fig. 3. Summary of differences in eyes, participant groups, and stimulus conditions. (*A*) Replotted data from Fig. 2 comparing waveforms across participant groups. The colors code the tested eyes. (*B*) Partial least squares analysis of multivariate spatiotemporal differences for *A* indicated two significant latent variables ($P < 0.0001$). (*Left*) Time courses for each latent variable with the time points of significant multivariate difference highlighted by black dots. Significant differences are present over the P1, N1, and L time periods. (*Right*) Weight patterns associated with the time courses (*Left*) (see text for details).

of visual acuity. Intact high-spatial frequency processing such as that reflected in letter-acuity tasks appears to be sufficient to produce a normal first LV in both test and control conditions in the dominant eyes of patients with anisometropic amblyopia, but not in patients with strabismic amblyopia.

The second LV weights were all negative in the test condition and mostly positive in the control conditions, indicating that this LV primarily reflects response differences between the test and control conditions (Fig. 3*B*, *Lower*). These differences were smallest between amblyopic eyes, reflecting the reduced IC-selective response seen in the time averages. Time points of significant difference associated with this pattern were present during the P1 period and a time period that spans the transition between the N1 and L peaks of the averaged response. Multivariate analysis thus reveals time courses of difference that are closely associated with the timing of ERP peaks in the case of the first LV and dissociated from them in the case of the second LV. The average responses shown in Figs. 2 and 3*B* are a composition of these two underlying processes. The individual subject "scalp" scores for the PLS analysis in Fig. 3*B* are provided in Fig. S1. The scalp scores represent the extent to which an individual participant expresses the pattern of weights for a given LV (51). The range of variability is comparable across groups and conditions, so the effects are not dominated by a small number of outliers.

Strabismic Patients Without Amblyopia. Because all of the participants with strabismic amblyopia had normal visual acuity in their dominant eyes, it is surprising to find abnormalities in their evoked responses. In addition to their amblyopia, these participants also had very poor or absent stereopsis. This raises the question of whether the dominant-eye abnormalities in strabismic amblyopia are related to the other eye's amblyopia (e.g., as a result of interocular interference), or whether they are related to other factors such as lack of normal binocular integration during early development. To address this question, we recorded ERP responses from 10 strabismic patients without amblyopia who had normal visual acuity (20/20–25 vision or better) in both eyes but who had strongly reduced or absent stereopsis.

Fig. 4 compares the evoked responses in strabismic patients with and without amblyopia. The responses from the dominant eye and the nondominant eye of strabismic patients without amblyopia are plotted in Fig. 4 (*Upper* and *Middle*, respectively). Fig. 4 (*Lower*) replots the responses from the dominant eyes of strabismic amblyopes from Fig. 2. As can be seen in Fig. 4, IC-selective responses during the N1 peak in both eyes of strabismic patients without amblyopia are similar to that of the dominant eyes of strabismic amblyopes. In other words, strabismic patients without amblyopia replicated the dominant-eye performance of strabismic amblyopia to IC stimuli.

Although nonamblyopic strabismic patients demonstrate IC-selective responses in both their dominant and nondominant eyes, their responses are abnormal, as can be seen when their responses are compared with those of normal-vision participants with fully functioning stereopsis (Fig. 5*A*). Compared with the participants with normal vision, strabismic patients without amblyopia have a general reduction in evoked-response amplitude in both test and control conditions. This reduction is especially apparent during the N1 component. We used the PLS approach to extract the latent structure underlying the multivariate responses and found two significant LVs ($P < 0.0001$ for the first LV and $P < 0.05$ for the second LV), as seen in Fig. 5*B*. The weight pattern of the first LV (Fig. 5*B*, *Upper Right*) indicates that this component reflects a common deficit in both test and control responses in both eyes of the patients, relative to both eyes of the normal controls. The time course of the first LV (Fig. 5*B*, *Upper Left*) shows the largest magnitude of difference during the time of the N1 peak of the averaged evoked response, as was seen in the multivariate comparison in Fig. 3*B* (*Left*). Differences between patients and controls thus increase at longer latencies at the N1 peak.

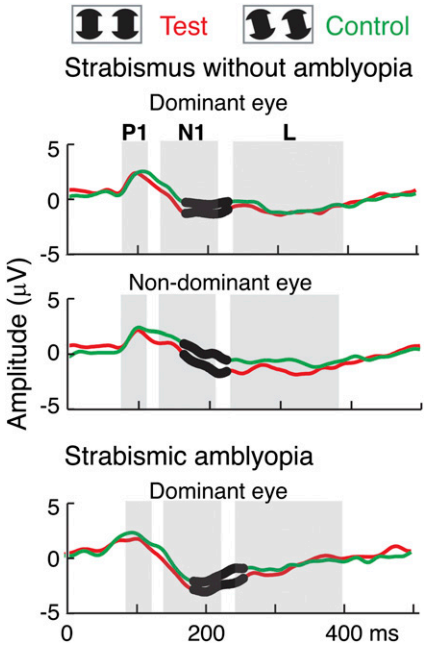

Fig. 4. Comparison of evoked responses in strabismic patients with and without amblyopia. The responses were averaged from both eyes of strabismic patients without amblyopia (*Upper* and *Middle*; $n = 10$) and the dominant eyes of strabismic amblyopes (*Lower*; replots from Fig. 2). The test condition (IC-present) is shown in red and the control condition (IC-absent) is in green. Black dots on the waveforms indicate the time points that were significantly different on permutation testing between test and control conditions ($P < 0.05$). IC-selective responses (differential responses to test vs. control conditions) during the N1 peak in both eyes of strabismic patients without amblyopia are similar to those of the dominant eyes of strabismic amblyopes.

The second LV time course (Fig. 5*B*, *Lower Left*) shows the time points of significant difference during the P1 peak of the averaged response and again during the transition between the N1 and L peaks. The weight pattern of the second LV (Fig. 5*B*, *Lower Right*) primarily reflects differences between test and control conditions, with these differences being of smaller magnitude in the patients than in the controls, as can be seen by the smaller difference between the positive and negative weights associated with the control and test stimuli, respectively. The individual subject scores from the PLS analysis of Fig. 5*B* are provided in Fig. S2. These results indicate that strabismus alone is sufficient to create strong abnormalities in the evoked response and that these abnormalities are independent of visual-acuity deficits, as both eyes of this group of patients had normal visual acuity.

Discussion

Two previously unidentified results have emerged from this study. First, strabismus generates significant abnormalities in both early and later stages of cortical processing, and these abnormalities are independent of visual-acuity deficits. Second, the visual processing in the normal-acuity nonamblyopic eyes of anisometropic amblyopes, by contrast, is normal, suggesting that these two forms of visual deprivation have different effects on early visual cortex.

Using stimuli that contain local motion and contrast cues as well as higher-order illusory contours, we found that the evoked responses from the normal-acuity dominant eye of patients with strabismic amblyopia and those from both eyes of strabismic

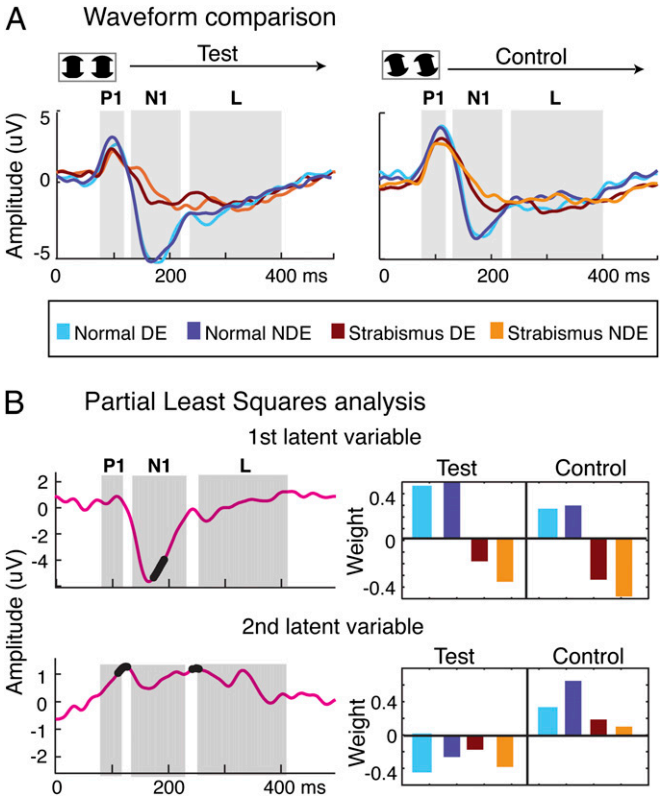

Fig. 5. Comparison of evoked responses between normal-vision participants and strabismic patients without amblyopia. (*A*) Waveform comparison across participant groups; data are replotted from Fig. 2 for normal participants and from Fig. 4 for strabismic patients without amblyopia. The colors code the tested eyes. DE, dominant eye; NDE, nondominant eye. (*B*) Partial least squares analysis for the data in *A* for the first latent variable (*Upper*; $P < 0.0001$) and the second latent variable (*Lower*; $P < 0.05$). (*Left*) Time courses for each latent variable with the time points of significant multivariate difference highlighted by black dots. Significant differences are present over the P1, N1, and L time periods. (*Right*) Weight patterns associated with the time courses (*Left*) (see text for details).

patients without acuity losses were abnormal during a phase of response that is before the time when IC sensitivity is first expressed. In contrast, the dominant-eye responses in the patients with anisometropic amblyopia were normal during this early time period and at a later time period when IC selectivity is formed. In normal-acuity eyes of strabismic patients with or without amblyopia, the deviation from the normal response pattern then increased during the later period of the response when IC configural activity is normally robust. Taken together, these results indicate that strabismus has an effect on both early and later stages of cortical processing, which is independent of any effect of reduced contrast sensitivity or spatial resolution. Disruptions of visual processing at this early stage may have had downstream consequences on the later, configuration-specific part of the response. Consistent with this, we also found that the amblyopic eyes of both strabismic and anisometropic amblyopes showed deficits over both the early and late time period of the evoked response. This result is less surprising given that the deficits in contrast sensitivity and spatial tuning properties, which are subtle in V1, become clearly manifest in V2 (17).

Our results in amblyopic eyes are broadly consistent with current thinking regarding the effects of deprivation on the development of visual cortex. Previous data from V1 of macaque models of amblyopia have suggested that, beyond a loss of binocular cells, there is insufficient difference between amblyopic and nonamblyopic eyes to explain the magnitude of behavioral losses in spatial contrast sensitivity (16, 17). This led to the notion that amblyopia is a consequence of cascading abnormalities in areas downstream of V1 (16). The first direct experimental evidence for this model comes from a recent study of deprivation in a macaque experimental strabismus model. Bi and coworkers (17) found that ocular dominance shifts strongly toward the unoperated eye in severe strabismic amblyopia in V2 but not in V1. Moreover, spatial tuning properties are measurably abnormal in V2 but not in V1. These results are consistent with the notion that behavioral amblyopia is the result of a cascading of loss over increasingly higher levels of visual processing. Bi and coworkers argued that the more severe effects of deprivation in V2 are due to suppressive interactions between eyes that begin in V1 and are also present in V2. The extent of suppression also correlated with behavioral amblyopia.

One of our contributions is to show that deprivation from strabismus has its effects earlier in this processing chain than the deprivation from chronic blur (anisometropia). The early part of the evoked response is abnormal in strabismus but normal in anisometropia. Importantly, the effect in strabismus is independent of losses in spatial sensitivity; for example, it is independent of amblyopia per se, which has historically been defined on the basis of a loss of visual acuity. Very little data is available on the relative effects of these two forms of deprivation in animal models. When these two forms of deprivation have been compared in macaque, no clear differences have been found in cell tuning at V1 (16, 45). To our knowledge, there has been no demonstration of deficits in the monocular properties of the fellow eyes in either anisometropic or strabismic amblyopia. Our work thus places the likely site of divergence between the behavioral phenotypes of these two forms of deprivation at an earlier rather than later stage of processing.

Beyond showing differences in the timing and magnitude of effects of the two types of deprivation on neural responses in humans, our results from the normal-acuity eyes of strabismic patients suggest that traditional ocular dominance histograms, which index the proportion of cells that can be driven by either eye (8), may not be particularly sensitive to the absolute level of monocular performance of the cells under test. A simple loss of binocular cells does not readily explain the loss of both early nonconfigural responses (at P1) and configural ones (at N1) in the dominant, fixating eye of strabismic amblyopes. A previous study has suggested that the primary deficit in V1 of strabismic animals is a loss of excitatory binocular interactions, combined with a pattern of abnormal binocular interaction. Therefore, the ratio of binocular to monocular response rates is reduced by deprivation (17). Bi and coworkers suggest that these disruptions of binocularity in V1 lead to abnormal development in downstream areas, such as at V2 (17). Our results suggest that the normal development of these processes and possibly others is necessary for complete development in early visual cortex, including nominally monocular response properties. Asymmetric suppression between the two eyes may exacerbate these losses and lead to the loss of spatial resolution that is the defining characteristic of amblyopia. The fact that the normal-acuity eye of strabismic patients with amblyopia develops the same deficit pattern as the two eyes of strabismic patients with no amblyopia, who typically have very strong, alternating (symmetric) suppression, further emphasizes the importance of intact binocular integration processes for normal development of form vision. Importantly, suppression prevents stereopsis, the perception of depth from horizontal disparity. Disparity tuning is strongly dependent on normal excitatory interaction, and excitatory inputs from the nonfixating eye are preferentially lost in strabismus (52–54).

Most of our anisometropic amblyopes had measurable stereopsis, but most of the patients with strabismus did not. Whereas the dominant eyes of patients with anisometropic or strabismic amblyopia each rarely, if ever, experience suppression, the

dominant eye of the anisometropic patients participates in some degree of binocular interaction. Preserved excitatory interactions in anisometropic amblyopia may thus be sufficient to promote normal development of responses in areas that are both before and after the stage at which IC extraction is performed. In the absence of suppression, these responses and later ones develop normally. In the case of strabismus, we propose that suppression eliminates excitatory binocular interactions that are essential for the complete development of both early and later stages of the visual pathway. Perhaps these interactions afford better development of the monocular response properties through an instructive role of correlated binocular interactions or an improved ability to develop scene-segmentation mechanisms under the guidance of stereoscopic cues for object and surface depths.

The Locus of Strabismic Deficits. A critical feature of our analysis is the use of the timing of the onset of IC-selective responses as a means of "locating" the acuity-independent deficit in strabismus. As noted in the introduction, the IC paradigm is attractive because the emergence of IC sensitivity is relatively well understood. In macaque, a reliable response to IC stimuli can first be recorded in V2 (31, 42, 43). IC and real contours produce similar activation in macaque V4 (55), and cells in IT of macaque are tuned for shapes defined by Kanisza-type ICs (55). IC selectivity has also been relatively well studied in humans (56). ERP studies have shown that ICs can modulate the first negative component (N1), peaking ~145–160 ms poststimulus onset (57–59). This effect appears to begin on the downward slope of the preceding P1, as can be seen in our data and in those of previous studies (49, 56, 60). Other studies using high-density ERPs combined with functional magnetic resonance imaging (fMRI) (49, 61, 62), high-density ERP alone (50, 58, 60, 63–65), magnetoencephalography (66), and fMRI alone (67, 68) suggest that IC-selective processing first occurs within higher-tier object-recognition areas of the lateral occipital complex (LOC) without a substantial contribution from earlier areas such as V1 or V2 (49, 58, 61, 62, 67–69) to the dominant effect at N1. Taken together, evidence from single-unit electrophysiology and functional neuroimaging studies in humans suggests that ICs are strongly represented in second-tier extrastriate cortex (e.g., LOC in humans, V4/IT in macaque), but that the first stages of this process may begin as early as V2. In our data, IC selectivity is first measurable on the downward slope of P1 at around 110 ms poststimulus. In the normal-acuity eyes of strabismic patients, the entire P1 response is depressed, including the portion of the response that occurs before IC sensitivity is first expressed. As just noted, there is evidence that IC selectivity may occur as early as V2, and we now know that the amblyopic deficit begins to be expressed more clearly in the properties of V2, possibly as a result of failed input from V1 (17). Our results are thus consistent with the strabismic deficit being due to a failure of transfer of information as early as from V1 to V2 (17). The IC task is more complex than the simple spatial-tuning task used to measure cell responses in V1 and V2, and may therefore be more sensitive to losses in the nonamblyopic eye. In our study, it is likely that P1 contains responses from both V1 and V2 and possibly V3. What is important about our results is that the response is abnormal as soon as we can measure it in strabismus. This places monocular aspects of the strabismic deficits early in the pathway at a stage of processing that is not affected by another common form of deprivation (anisometropia) in humans.

Visual Deficits in the Fellow Eye of Amblyopes. Visual deficits in the normal-acuity fellow eyes of patients with amblyopia have been reported previously in psychophysical studies. These fellow-eye abnormalities have been found in motion-discrimination tasks (27, 70, 71), global form tasks (19, 21, 72, 73), and second-order target-detection tasks (74). These deficits are more common in the fellow eyes of strabismic amblyopes than in anisometropic fellow eyes (75), but have also been noted in some tasks in anisometropia (22, 70). The most pronounced fellow-eye deficits reported in the fellow eye of anisometropes are in a contour-in-noise task in a macaque model (22) and in a motion-defined form task in human children (70, 76). These tasks each involved the integration of noisy local measurements of orientation or motion into a global percept and are thus quite different from the task we have studied. Deficits are also found in both eyes of strabismic patients with no amblyopia, as we find here. These bilateral deficits in strabismus have been reported in a contour-integration task (21) and in a related second-order flanker task (74).

Our results shed new light on these previous psychophysical studies. These studies interpreted the failures as being due to selective losses in extrastriate areas. The basis for this inference was an assumption that early visual processing was normal because acuity was normal (in nonamblyopic eyes) or because the stimuli were equated for low-level feature visibility (in amblyopic eyes). These inferences are necessarily indirect. By studying the temporal evolution of the ERP, a direct measure of neural activity, we have shown that even the earliest stages of visual processing, as manifest in the P1 peak, are affected in the normal-acuity nonamblyopic eyes of strabismic patients but not in the nonamblyopic eyes of anisometropes. This suggests that the strabismic deficit begins very early in cortex, is present in both eyes, and is not related to visual-acuity loss. The amblyopic deficit increases at later time points/high-cortical areas in both types of amblyopia. The two types of patients thus differ in the initial site of abnormality, but both types demonstrate increasing levels of deficit in the higher level of visual processing that is tapped by the late activity in our IC task.

Materials and Methods

Participants. A total of 40 adult observers (20–66 y old) participated. All normal-vision observers (n = 10) were individually age-matched to amblyopic and strabismic observers within 20% of their age. Observers with a history of anisometropic amblyopia (n = 10), strabismic amblyopia (n = 10), and strabismus without amblyopia (n = 10) participated. All participants were refracted under noncycloplegic conditions by a pediatric ophthalmologist before the experiments. All patients were screened for the presence of monocular fixation instability and eccentric fixation using a direct ophthalmoscope. Participants who had eccentric fixation and nystagmus or latent nystagmus (nystagmus that appears when covering one eye) were excluded from the study. Visual acuity was evaluated with a LogMAR chart (Bailey–Lovie) and was measured with best optical correction. Stereoacuity was measured with Randot stereotests (Stereo Optical) at a near distance with best optical correction. All normal-vision observers had 20/20 or better optotype acuity in each eye and stereoacuity of at least 30 arc·s. They also had no prior history of strabismus, amblyopia, or any other eye diseases.

Patient participants were classified into three groups: (*i*) anisometropic amblyopia: Amblyopic observers with unequal refractive error between the two eyes of at least 1 diopter in any meridian and with no constant ocular deviation or history of strabismus surgery; (*ii*) strabismic amblyopia: Amblyopic observers with a constant ocular deviation or a history of prior strabismus surgery with or without anisometropia; and (*iii*) strabismus without amblyopia: Strabismic patients who had equal acuity that was better than 20/25 in each eye. All patient participants had no history of other eye diseases (e.g., cataract, ptosis, glaucoma, lens implant, etc.). The two amblyopic groups had similar visual-acuity distributions, with mean visual acuity of 20/83 (SD 20/50) and 20/80 (SD 20/63) for eyes with anisometropic and strabismic amblyopia, respectively (P = 0.8). However, most of the anisometropic amblyopes had relatively good stereopsis (i.e., between 50 and 200 arc second) or residual stereopsis (i.e., between 200 and 400 arc second). In most of the strabismic amblyopes and strabismic patients without amblyopia, stereopsis was not measurable using Randot stereotests with 2,000 arc second as the maximum measurable stereoacuity. Refractive errors were corrected for the testing distance (70 cm) in all observers during the experiments. Clinical details of the observers with amblyopia and strabismus are shown in Table 1.

The research protocol was approved by the Institutional Review Board of the California Pacific Medical Center and conformed to the tenets of the

Declaration of Helsinki. Written informed consent was obtained after the ERP recording procedure was explained.

Stimuli. Illusory contours were generated in a display composed of an array of black, notched circles (inducers) on a white background (Fig. 1*A*). There were 45 inducers arranged in 5 rows with 9 inducers in each row. The inducers were separated from their neighbors by 2.86° horizontally (along rows) and 3.68° vertically (along columns). Each inducer spanned 2.5° of visual angle. When the inducers were aligned (0°), there were 40 illusory rectangles (IC-present). Each illusory rectangle subtended 1.6° × 1.5°. When the inducers were misaligned (e.g., 20°, 50°, and 70° offset from alignment), the illusory rectangles disappeared (IC-absent) (Fig. 1*B*). The stimuli were presented on a color CRT monitor (Mitsubishi; Diamond Pro 2070) running in monochrome mode (black inducers on a white background). The display was set at an 800 × 600-pixel resolution and a 72-Hz refresh rate. It was positioned at 70 cm, generating a 27° by 18° visual field. The mean luminance of the background was constant at 125 cd/m^2. The contrast of inducers was 90% (Michelson definition).

Perceptual Reports. A perceptual report was elicited from each eye of the patients by asking them to compare spatially filtered and unfiltered ICs across their two eyes. A reference IC target (Fig. 1*A*) was blurred using the Photoshop Gaussian blur tool at four levels, with each level adding 1 pixel additional radius to the filter (1 pixel equals 0.007 arc·min). Patients first viewed the unfiltered image with their dominant (fellow) eye and then with their nondominant (amblyopic eye). They were then asked to choose the filtered image viewed by their fellow eye that best matched their percept of the unfiltered image shown to their amblyopic eye. Patients reported clear IC percepts when viewing with their fellow eyes in the case of patients with amblyopia and in both eyes in patients without amblyopia. The matches to the amblyopic eye percepts spanned a range of blur levels. Among the 20 amblyopic eyes, 9 matches occurred at level 1 of blur, 6 at level 2, and 5 at level 3. None of the participants used the level 4 blurred image as a match.

ERP Recording. Grass E-6H gold-cup surface electrodes were used to collect EEG data. The EEG was amplified at a gain of 50,000, with amplitude band pass-filter settings of 0.3–100 Hz (model 12BIN/8CH-23C; Grass Instruments). Five active electrodes were placed over the occipital pole at PO_7, O_1, O_Z, O_2, and PO_8 of the International 10-20 system (77). The reference and ground electrodes were placed at C_Z and P_Z, respectively. Impedance was measured and maintained between 3 and 10 kΩ. The EEG was digitized to a nominal 16-bit accuracy at a sampling rate of 432 Hz via a National Instruments PCI-MIO16XE-50 card controlled by in-house software that also performed signal processing and user-interface functions. The observers were instructed to fixate on a small fixation point in the center of the monitor. Viewing was monocular for all observers, with the nonviewing eye occluded with a black eye patch during the experiment. An ERP recording session consisted of 10 trials per condition and per eye for all observers. Each trial lasted 12 s, with the first and last seconds being discarded. The same stimulus condition was repeated 100 times.

Table 1. Clinical details of the patients

	Visual acuity			Refractive errors		
Patient	Dominant eye	Nondominant eye	Ocular alignment	Dominant eye	Nondominant eye	Stereoacuity, arc second
1	20/20	20/50–1	ortho-XT 6pd	+3.00	+5.50+0.50*15	NA
2	20/16–1	20/50+3	ortho	plano	+1.50+1.00*65	70
3	20/20–3	20/50+1	ortho	−1.00	−5.50+0.50*40	NA
4	20/20	20/50	ortho	+0.50	+0.50+2.00*180	70
5	20/20	20/60	ortho	−0.25	+3.00+0.50*90	340
6	20/16–1	20/63+1	ortho	plano	+3.50+0.50*140	400
7	20/20+1	20/63–1	ortho	−0.50+0.50*90	−1.00+3.00*90	400
8	20/20–1	20/125	ortho	+2.00+1.00*70	+4.00+2.00*110	400
9	20/12.5	20/125	ortho	plano	+3.00+2.50*140	200
10	20/20	20/200	ortho	+6.00–2.00*25	+7.50–2.50*180	NA
11	20/20	20/40	ET 15pd, DVD	−6.00	−6.00	NA
12	20/20–3	20/40+3	XT 2pd	+4.00+1.00*10	+2.00+1.00*170	NA
13	20/20–1	20/50–2	ET 40pd, L/R 6pd	plano-1.50*140	+2.25–2.50*20	NA
14	20/20	20/50	XT 8–12pd, L/R 5pd	−5.25	−12.25	200
15	20/20–1	20/40+2	ortho-exophoria	−1.00–0.50*170	−0.75–0.50*30	NA
16	20/20+2	20/63+2	XT 16pd, R/L 6pd	−4.00+1.00*90	−3.50+1.50*90	NA
17	20/20+2	20/80–2	XT 12pd, R/L 4pd	−0.50+ 0.50*140	−9.00–1.00*50	NA
18	20/16–2	20/80+3	ET 6pd, R/L 8pd	−2.25–2.00*175	−16.5–4.00*172	NA
19	20/12.5–2	20/100–2	ET 3pd, L/R 3pd	+3.00–0.75*110	+3.25–1.25*80	NA
20	20/20+2	20/250	XT 6pd	−0.50–1.25*90	+4.00+2.00*90	NA
21	20/16–2	20/20	XT 12–14pd	plano	+1.00	200
22	20/16+2	20/25–2	ET 8pd, L/R 16–20pd	plano	+2.00+0.25*100	NA
23	20/20+2	20/20+1	ET 10pd	−4.25–0.50*170	−4.75–0.75*170	NA
24	20/16–1	20/20–2	ET 6pd, L/R 2pd	+2.25+0.75*20	+3.00+0.50*20	NA
25	20/20	20/16–1	ET 16pd	−1.50+ 0.50*110	−1.00–0.25*110	NA
26	20/16–1	20/25	XT 4pd, L/R 4pd	+0.25+ 1.00*100	+3.25+1.25*100	340
27	20/16–2	20/20+2	ET 30pd, R/L 8pd	plano-1.00*80	+0.50	NA
28	20/16–2	20/20–2	XT 4–6pd	+3.50+ 0.50*140	+1.00	NA
29	20/20+2	20/25–1	ET 40pd, L/R 6pd	−2.00+ 0.75*145	+0.50+0.25*105	NA
30	20/20–1	20/25+1	XT 20pd, L/R 8pd	−0.50–2.00*90	−2.00	NA

Patients 1–10 are anisometropic amblyopia; 11–20 are strabismic amblyopia; and 21–30 are strabismus without amblyopia. Stereoacuity was measured at near distance. Stereoauity marked "NA" indicates nonmeasurable stereoacuity. Ocular alignment at near with correction is shown in prism diopters. DVD, disassociated vertical deviation; ET, esotropia; L/R, left-eye hypertropia; R/L, right-eye hypertropia; XT, exotropia.

ERP Analysis. The data in Figs. 2, 3*A*, 4, and 5*A* were obtained by spectral decomposition and back-reconstruction to the time domain (waveform). For each subject, stimulus condition, and electrode derivation, raw recordings for each trial were partitioned into five sequential epochs. These epochs were averaged together within each trial and then across trials to obtain a single grand average waveform for each observer, derivation, and stimulus condition. Each grand average waveform was decomposed by discrete Fourier transformation and digitally filtered by zeroing the data at 53 Hz and above to remove 60-Hz and other high-frequency noise. A new waveform corresponding to a single stimulus cycle (1-s duration) was then reconstructed by inverse discrete Fourier transformation of this filtered spectrum. These reconstructed waveforms were then averaged together across observers for each derivation and stimulus condition. All of the figures show the data after the second transition (500-ms duration) of a 1,000-ms single stimulus cycle. This time point is marked "0 ms" in the figures.

Statistical Analysis. Conventional time-locked averages were computed over the 1,000-ms stimulus cycle. The statistical reliability of the difference at each time point between two waveforms (Figs. 2 and 4) was tested using permutation methods (78, 79). Under the null hypothesis of no difference between two conditions, the two response waveforms are exchangeable for a given subject. By randomly permuting which subjects had their waveforms exchanged, we created a large set of permuted datasets. For each permutation, we calculated the *t* value (10 degrees of freedom) for each time point in the waveform. Then, the maximum *t* values from each permutation were accumulated into a reference distribution. Any time point from the original, unexchanged data whose *t* value fell within the top fifth percentile of the reference distribution was deemed significant and implied rejection of the null hypothesis with a 5% probability of type 1 (false rejection) error. Such time points in the waveform plots in Figs. 2 and 4 are indicated with black dots.

The primary analyses were conducted using partial least squares as described by Lobaugh et al. (51) (Figs. 3*B* and 5*B*). PLS is a multivariate technique, similar to factor analysis, that nonparametrically estimates significance of LVs. It can be used to systematically summarize differences between experimental conditions in terms of spatial (e.g., amplitude) and temporal (e.g., latency) variables. After computing a mean waveform across subjects for each relevant stimulus condition, we subtract the mean for each condition from the mean across all conditions. The resulting deviation waveforms for each condition are gathered into a matrix, which is then subjected to singular-value decomposition to determine the LVs in the deviation matrix. Each LV consists of three parts: (*i*) a waveform vector that represents the manifestation of the latent effect in time domain; (*ii*) a corresponding vector that represents the loading of each condition on this latent waveform; and (*iii*) a scalar singular value indicating the relative weight contributed by the latent effect to the deviation matrix. Significance of LV singular values was obtained by permutation testing; for example, significance of PLS waveforms was obtained by resampling from the subjects in the original sample.

ACKNOWLEDGMENTS. The authors thank Suzanne McKee and Faraz Farzin for discussions and comments on the manuscript and Margaret Q. McGovern for her assistance in recruiting the participants. Supported by The Smith-Kettlewell Eye Research Institute, the West China Hospital Fund, and National Institutes of Health Grant EY06759.

1. Knudsen EI (2004) Sensitive periods in the development of the brain and behavior. *J Cogn Neurosci* 16(8):1412–1425.
2. Berardi N, Pizzorusso T, Maffei L (2000) Critical periods during sensory development. *Curr Opin Neurobiol* 10(1):138–145.
3. Hubel DH, Wiesel TN (1977) Ferrier lecture. Functional architecture of macaque monkey visual cortex. *Proc R Soc Lond B Biol Sci* 198(1130):1–59.
4. Espinosa JS, Stryker MP (2012) Development and plasticity of the primary visual cortex. *Neuron* 75(2):230–249.
5. Ciuffreda J, Levi DM, Selenow A (1991) *Amblyopia: Basic and Clinical Aspects* (Butterworth-Heinemann, Boston).
6. Barrett BT, Bradley A, McGraw PV (2004) Understanding the neural basis of amblyopia. *Neuroscientist* 10(2):106–117.
7. Levi DM (2006) Visual processing in amblyopia: Human studies. *Strabismus* 14(1): 11–19.
8. Kiorpes L (2006) Visual processing in amblyopia: Animal studies. *Strabismus* 14(1): 3–10.
9. Wiesel TN, Hubel DH (1963) Single-cell responses in striate cortex of kittens deprived of vision in one eye. *J Neurophysiol* 26(6):1003–1017.
10. Muir DW, Mitchell DE (1973) Visual resolution and experience: Acuity deficits in cats following early selective visual deprivation. *Science* 180(4084):420–422.
11. Antonini A, Stryker MP (1993) Rapid remodeling of axonal arbors in the visual cortex. *Science* 260(5115):1819–1821.
12. Hubel DH, Wiesel TN (1965) Binocular interaction in striate cortex of kittens reared with artificial squint. *J Neurophysiol* 28(6):1041–1059.
13. von Noorden GK, Crawford ML (1978) Morphological and physiological changes in the monkey visual system after short-term lid suture. *Invest Ophthalmol Vis Sci* 17(8): 762–768.
14. Crawford ML (1978) The visual deprivation syndrome. *Ophthalmology* 85(5):465–477.
15. Movshon JA, et al. (1987) Effects of early unilateral blur on the macaque's visual system. III. Physiological observations. *J Neurosci* 7(5):1340–1351.
16. Kiorpes L, Kiper DC, O'Keefe LP, Cavanaugh JR, Movshon JA (1998) Neuronal correlates of amblyopia in the visual cortex of macaque monkeys with experimental strabismus and anisometropia. *J Neurosci* 18(16):6411–6424.
17. Bi H, et al. (2011) Neuronal responses in visual area V2 (V2) of macaque monkeys with strabismic amblyopia. *Cereb Cortex* 21(9):2033–2045.
18. Popple AV, Levi DM (2000) Amblyopes see true alignment where normal observers see illusory tilt. *Proc Natl Acad Sci USA* 97(21):11667–11672.
19. Chandna A, Pennefather PM, Kovács I, Norcia AM (2001) Contour integration deficits in anisometropic amblyopia. *Invest Ophthalmol Vis Sci* 42(3):875–878.
20. Hess RF, McIlhagga W, Field DJ (1997) Contour integration in strabismic amblyopia: The sufficiency of an explanation based on positional uncertainty. *Vision Res* 37(22): 3145–3161.
21. Kovács I, Polat U, Pennefather PM, Chandna A, Norcia AM (2000) A new test of contour integration deficits in patients with a history of disrupted binocular experience during visual development. *Vision Res* 40(13):1775–1783.
22. Kozma P, Kiorpes L (2003) Contour integration in amblyopic monkeys. *Vis Neurosci* 20(5):577–588.
23. Levi DM (2008) Crowding—An essential bottleneck for object recognition: A minireview. *Vision Res* 48(5):635–654.
24. Hou C, Pettet MW, Norcia AM (2008) Abnormalities of coherent motion processing in strabismic amblyopia: Visual-evoked potential measurements. *J Vis* 8(4):1–12.
25. Simmers AJ, Ledgeway T, Mansouri B, Hutchinson CV, Hess RF (2006) The extent of the dorsal extra-striate deficit in amblyopia. *Vision Res* 46(16):2571–2580.
26. Simmers AJ, Ledgeway T, Hess RF (2005) The influences of visibility and anomalous integration processes on the perception of global spatial form versus motion in human amblyopia. *Vision Res* 45(4):449–460.
27. Simmers AJ, Ledgeway T, Hess RF, McGraw PV (2003) Deficits to global motion processing in human amblyopia. *Vision Res* 43(6):729–738.
28. Ho CS, Giaschi DE (2006) Deficient maximum motion displacement in amblyopia. *Vision Res* 46(28):4595–4603.
29. Sharma V, Levi DM, Klein SA (2000) Undercounting features and missing features: Evidence for a high-level deficit in strabismic amblyopia. *Nat Neurosci* 3(5):496–501.
30. Tripathy SP, Levi DM (2008) On the effective number of tracked trajectories in amblyopic human vision. *J Vis* 8(4):1–22.
31. Lee TS, Nguyen M (2001) Dynamics of subjective contour formation in the early visual cortex. *Proc Natl Acad Sci USA* 98(4):1907–1911.
32. Nieder A, Wagner H (1999) Perception and neuronal coding of subjective contours in the owl. *Nat Neurosci* 2(7):660–663.
33. Peterhans E, von der Heydt R (1991) Subjective contours—Bridging the gap between psychophysics and physiology. *Trends Neurosci* 14(3):112–119.
34. Cox MA, et al. (2013) Receptive field focus of visual area V4 neurons determines responses to illusory surfaces. *Proc Natl Acad Sci USA* 110(42):17095–17100.
35. Kanizsa G (1979) *Organization in Vision: Essays on Gestalt Perception* (Praeger, New York).
36. Marr D (1982) *Vision: A Computational Investigation into the Human Representation and Processing of Visual Information* (W.H. Freeman, New York).
37. De Weerd P, Desimone R, Ungerleider LG (1996) Cue-dependent deficits in grating orientation discrimination after V4 lesions in macaques. *Vis Neurosci* 13(3):529–538.
38. Merigan WH (1996) Basic visual capacities and shape discrimination after lesions of extrastriate area V4 in macaques. *Vis Neurosci* 13(1):51–60.
39. Huxlin KR, Merigan WH (1998) Deficits in complex visual perception following unilateral temporal lobectomy. *J Cogn Neurosci* 10(3):395–407.
40. Huxlin KR, Saunders RC, Marchionini D, Pham HA, Merigan WH (2000) Perceptual deficits after lesions of inferotemporal cortex in macaques. *Cereb Cortex* 10(7): 671–683.
41. McKee SP, Levi DM, Movshon JA (2003) The pattern of visual deficits in amblyopia. *J Vis* 3(5):380–405.
42. von der Heydt R, Peterhans E, Baumgartner G (1984) Illusory contours and cortical neuron responses. *Science* 224(4654):1260–1262.
43. Peterhans E, von der Heydt R (1989) Mechanisms of contour perception in monkey visual cortex. II. Contours bridging gaps. *J Neurosci* 9(5):1749–1763.
44. Levi DM, Klein S (1982) Hyperacuity and amblyopia. *Nature* 298(5871):268–270.
45. Crawford ML, Harwerth RS (2004) Ocular dominance column width and contrast sensitivity in monkeys reared with strabismus or anisometropia. *Invest Ophthalmol Vis Sci* 45(9):3036–3042.
46. Smith EL III, et al. (1997) Residual binocular interactions in the striate cortex of monkeys reared with abnormal binocular vision. *J Neurophysiol* 78(3):1353–1362.
47. El-Shamayleh Y, Kiorpes L, Kohn A, Movshon JA (2010) Visual motion processing by neurons in area MT of macaque monkeys with experimental amblyopia. *J Neurosci* 30(36):12198–12209.
48. Norcia AM, Sampath V, Hou C, Pettet MW (2005) Experience-expectant development of contour integration mechanisms in human visual cortex. *J Vis* 5(2):116–130.

49. Murray MM, et al. (2002) The spatiotemporal dynamics of illusory contour processing: Combined high-density electrical mapping, source analysis, and functional magnetic resonance imaging. *J Neurosci* 22(12):5055–5073.
50. Foxe JJ, Murray MM, Javitt DC (2005) Filling-in in schizophrenia: A high-density electrical mapping and source-analysis investigation of illusory contour processing. *Cereb Cortex* 15(12):1914–1927.
51. Lobaugh NJ, West R, McIntosh AR (2001) Spatiotemporal analysis of experimental differences in event-related potential data with partial least squares. *Psychophysiology* 38(3):517–530.
52. Sengpiel F, Blakemore C (1994) Interocular control of neuronal responsiveness in cat visual cortex. *Nature* 368(6474):847–850.
53. Chino YM, Smith EL III, Yoshida K, Cheng H, Hamamoto J (1994) Binocular interactions in striate cortical neurons of cats reared with discordant visual inputs. *J Neurosci* 14(8): 5050–5067.
54. Scholl B, Tan AY, Priebe NJ (2013) Strabismus disrupts binocular synaptic integration in primary visual cortex. *J Neurosci* 33(43):17108–17122.
55. Pan Y, et al. (2012) Equivalent representation of real and illusory contours in macaque V4. *J Neurosci* 32(20):6760–6770.
56. Murray MM, Herrmann CS (2013) Illusory contours: A window onto the neurophysiology of constructing perception. *Trends Cogn Sci* 17(9):471–481.
57. Herrmann CS, Bosch V (2001) Gestalt perception modulates early visual processing. *Neuroreport* 12(5):901–904.
58. Pegna AJ, Khateb A, Murray MM, Landis T, Michel CM (2002) Neural processing of illusory and real contours revealed by high-density ERP mapping. *Neuroreport* 13(7):965–968.
59. Proverbio AM, Zani A (2002) Electrophysiological indexes of illusory contours perception in humans. *Neuropsychologia* 40(5):479–491.
60. Murray MM, Foxe DM, Javitt DC, Foxe JJ (2004) Setting boundaries: Brain dynamics of modal and amodal illusory shape completion in humans. *J Neurosci* 24(31):6898–6903.
61. Ritzl A, et al. (2003) Functional anatomy and differential time courses of neural processing for explicit, inferred, and illusory contours. An event-related fMRI study. *Neuroimage* 19(4):1567–1577.
62. Kruggel F, Herrmann CS, Wiggins CJ, von Cramon DY (2001) Hemodynamic and electroencephalographic responses to illusory figures: Recording of the evoked potentials during functional MRI. *Neuroimage* 14(6):1327–1336.
63. Shpaner M, Murray MM, Foxe JJ (2009) Early processing in the human lateral occipital complex is highly responsive to illusory contours but not to salient regions. *Eur J Neurosci* 30(10):2018–2028.
64. Murray MM, Imber ML, Javitt DC, Foxe JJ (2006) Boundary completion is automatic and dissociable from shape discrimination. *J Neurosci* 26(46):12043–12054.
65. Knebel JF, Murray MM (2012) Towards a resolution of conflicting models of illusory contour processing in humans. *Neuroimage* 59(3):2808–2817.
66. Halgren E, Mendola J, Chong CD, Dale AM (2003) Cortical activation to illusory shapes as measured with magnetoencephalography. *Neuroimage* 18(4):1001–1009.
67. Mendola JD, Dale AM, Fischl B, Liu AK, Tootell RB (1999) The representation of illusory and real contours in human cortical visual areas revealed by functional magnetic resonance imaging. *J Neurosci* 19(19):8560–8572.
68. Stanley DA, Rubin N (2003) fMRI activation in response to illusory contours and salient regions in the human lateral occipital complex. *Neuron* 37(2):323–331.
69. Brighina F, et al. (2003) Illusory contours and specific regions of human extrastriate cortex: Evidence from rTMS. *Eur J Neurosci* 17(11):2469–2474.
70. Ho CS, et al. (2005) Deficient motion perception in the fellow eye of amblyopic children. *Vision Res* 45(12):1615–1627.
71. Giaschi DE, Regan D, Kraft SP, Hong XH (1992) Defective processing of motion-defined form in the fellow eye of patients with unilateral amblyopia. *Invest Ophthalmol Vis Sci* 33(8):2483–2489.
72. Simmers AJ, Bex PJ (2004) The representation of global spatial structure in amblyopia. *Vision Res* 44(5):523–533.
73. Husk JS, Hess RF (2013) Global processing of orientation in amblyopia. *Vision Res* 82: 22–30.
74. Wong EH, Levi DM, McGraw PV (2005) Spatial interactions reveal inhibitory cortical networks in human amblyopia. *Vision Res* 45(21):2810–2819.
75. Hess RF, Demanins R (1998) Contour integration in anisometropic amblyopia. *Vision Res* 38(6):889–894.
76. Wang J, Ho CS, Giaschi DE (2007) Deficient motion-defined and texture-defined figure-ground segregation in amblyopic children. *J Pediatr Ophthalmol Strabismus* 44(6):363–371.
77. Odom JV, et al. (2010) ISCEV standard for clinical visual evoked potentials (2009 update). *Doc Ophthalmol* 120(1):111–119.
78. Blair RC, Karniski W (1993) An alternative method for significance testing of waveform difference potentials. *Psychophysiology* 30(5):518–524.
79. Nichols TE, Holmes AP (2002) Nonparametric permutation tests for functional neuroimaging: A primer with examples. *Hum Brain Mapp* 15(1):1–25.